THE JOURNAL OF PHYSICAL CHEMISTRY B

Article

Cite This: J. Phys. Chem. B 2018, 122, 3354−3362

pubs.acs.org/JPCB

Interfacial Tension of Phase-Separated Polydisperse Mixed Polymer Solutions

Mark Vis,*[,†] Edgar M. Blokhuis,[‡] Ben H. Erné,[§] R. Hans Tromp,[§,∥] and Henk N. W. Lekkerkerker[§]

[†]Laboratory of Physical Chemistry, Department of Chemical Engineering and Chemistry & Institute for Complex Molecular Systems, Eindhoven University of Technology, P.O. Box 513, 5600 MB Eindhoven, The Netherlands

[‡]Colloid and Interface Science, Gorlaeus Laboratories, Leiden Institute of Chemistry, P.O. Box 9502, 2300 RA Leiden, The Netherlands

[§]Van 't Hoff Laboratory for Physical and Colloid Chemistry, Debye Institute for Nanomaterials Science, Utrecht University, Padualaan 8, 3584 CH Utrecht, The Netherlands

[∥]NIZO food research, Kernhemseweg 2, 6718 ZB Ede, The Netherlands

ABSTRACT: Aqueous two-phase systems provide oil-free alternatives in the formulation of emulsions in food and other applications. Theoretical interpretation of measurements on such systems, however, is complicated by the high polydispersity of the polymers. Here, phase diagrams of demixing and interfacial tensions are determined for aqueous solutions of two large polymers present in a mass ratio of 1:1, dextran (70 kDa) and nongelling gelatin (100 kDa), with or without further addition of smaller dextran molecules (20 kDa). Both in experiments and in calculations from Scheutjens−Fleer self-consistent field lattice theory, we find that small polymers decrease the interfacial tension at equal tie-line length in the phase diagram. After identifying the partial contributions of all chemical components to the interfacial tension, we conclude that excess water at the interface is partially displaced by small polymer molecules. An interpretation in terms of the Gibbs adsorption equation provides an instructive way to describe effects of polydispersity on the interfacial tension of demixed polymer solutions.

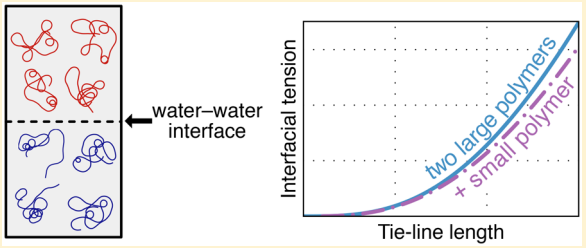

INTRODUCTION

In their monograph *Molecular Theory of Capillarity* first published in 1982,[1] Rowlinson and Widom address the crucial role played by the experimentally well-known phenomenon of interfacial tension in showing the existence of molecules and the forces between them. The monograph highlights the historic role played by van der Waals in the development of a theoretical description, first, in 1873, by the van der Waals equation of state quantifying these intermolecular forces[2] and second, 20 years later, by the introduction of the squared-gradient theory to provide means to determine the structure and tension of the interface.[3,4] More than a century later, squared-gradient theory and its mean-field extensions derived from density functional theory[5] are still commonly used in present day theoretical research on interfaces.[6]

An important class of interfaces that are currently of experimental and theoretical interest are those formed between phase-separated polymer blends and polymer solutions.[7,8] This is especially the case for the phase-separated polymer solutions that are encountered in daily life, such as in processed food, paint, and cosmetics. In recent years, such (aqueous) polymer systems have been the focus of considerable research efforts,[9,10] since control over their microstructure could result in obtaining aqueous substitutes for oil-containing food formulations. Improved control is necessary for long-term stability of water-in-water emulsions and to endow them with sensory quality. However, since these water−water interfaces usually have a very low interfacial tension (of the order of 10 μN m^{-1} or less),[11−14] with an interfacial thickness on the order of the polymer radius of gyration, adsorption of colloidal particles or small molecules is severely hampered.[15,16]

An important factor in all studies on phase-separated polymer solutions is the polymer chain length and its influence on the magnitude of the interfacial tension.[8,17,18] Not only is the investigation of the chain length dependence of theoretical interest, with particular attention on the scaling behavior as the chain length increases,[19−21] but it is also key in experiments, as chain length polydispersity is almost always a factor and many studies have addressed the phase composition of polydisperse systems.[22−26] In polydisperse mixtures, not all molecular size fractions are fractionated over the coexisting phases to the same degree. In particular, for the low molar mass fractions, the degree of fractionation over the phases is expected to be low. As a consequence, the interfacial tension is expected to be lowered (relative to the monodisperse case) when small molar mass fractions are present. Polydispersity may therefore provide a

Special Issue: Benjamin Widom Festschrift

Received: October 9, 2017
Revised: December 19, 2017
Published: December 19, 2017

DOI: 10.1021/acs.jpcb.7b09967
J. Phys. Chem. B 2018, 122, 3354−3362

way to modify the stability of water-in-water emulsions. Predicting the effect of polydispersity is, however, not simple, and the situation is complicated by the fact that water accumulates at the interface.[27]

In this work, we aim to understand better the influence of polydispersity on interfacial tension. The interfacial tension of a model system for a water-based food formulation is measured with and without the presence of a small molar mass fraction of one of the phase separating polymers. We compare our experimental results with self-consistent field lattice theory calculations.[28] Finally, an attempt is made to interpret our results in terms of the Gibbs adsorption equation for the various components.

METHODS

Experimental Details. *Sample Preparation.* Experiments were performed on aqueous mixtures of dextran and gelatin. Two different dextrans were used, with M_w = 70 kDa (Sigma-Aldrich, from *Leuconostoc* spp., "narrow molecular weight distribution" grade, product no. 44886, M_w/M_n = 1.72) and M_w = 15−25 kDa (Sigma-Aldrich, from *Leuconostoc* spp., product no. 31387). For brevity, these will be denoted from here on as "70 kDa dextran" and "20 kDa dextran". Gelatin of approximately 100 kDa (Norland products, from cold water fish, nongelling at room temperature, gelation temperature 8−10 °C, high molar mass grade,[29] $M_w/M_n \sim 2$) was kindly supplied by FIB Foods B.V. (Harderwijk, The Netherlands). The polymers were used as received. The polymer content of solutions will be expressed as mass fractions.

Stock solutions of the polymers were prepared as follows. Dextran was dissolved in Milli-Q water by gentle mixing on a roller bank. Two dextran stock solutions were prepared, one containing only dextran of 70 kDa (10%) and the other containing both 70 and 20 kDa dextran at 10 and 5%, respectively (2:1 polymer mass ratio). Gelatin was dissolved at 10% in Milli-Q water under magnetic stirring by heating in a water bath of approximately 60 °C for about 15−30 min until all material was dissolved and then allowed to cool to room temperature.

Samples were prepared by mixing the stock solutions and diluting with Milli-Q water. A 1:1 polymer mass ratio was used for samples containing 70 kDa dextran and gelatin and a ratio of 2:1:2 for samples containing 70 kDa dextran, 20 kDa dextran, and gelatin. The concentration of the two large polymers was varied in the range from 3.4 to 5.0%. The resulting samples were of approximately neutral pH and had a salt concentration of the order of 10 mM, due to residual salt from the polymers. Samples above the critical demixing concentration became turbid after mixing due to the onset of phase separation. Centrifugation overnight at 200 × *g* resulted in samples with two clear phases.

Phase Composition. After centrifugation, part of each phase was isolated. The composition of each phase was measured using polarimetry[30] at four wavelengths (589, 546, 436, and 365 nm) on an Anton Paar MCP 500 polarimeter, allowing simultaneous determination of the concentration of dextran and gelatin of each isolated phase. For an elaborate description of the procedure, see ref 31. We verified that the specific rotation of dextran is independent of molar mass; thereby, our measurements on systems containing both 20 and 70 kDa dextran yield their combined mass fraction in each phase. These measurements allow construction of phase diagrams and computation of the tie-line length defined in terms of the difference in polymer mass fraction between the two phases

$$L \equiv [(w_A^\alpha - w_A^\beta)^2 + (w_B^\alpha - w_B^\beta)^2]^{1/2} \quad (1)$$

where w_i^j indicates the (total) mass fraction of dextran (A) or gelatin (B) in each phase (denoted α and β).

Interfacial Tension. The interfacial tension γ of the water−water interface was obtained by measuring the capillary length

$$l_c \equiv [\gamma/\Delta\rho g]^{1/2} \quad (2)$$

where $\Delta\rho$ is the mass density difference between the two phases and g is the gravitational acceleration. The capillary length, in turn, was found by analyzing the deformation of the static interfacial profile near a vertical wall,[32] which has a shape given by[33]

$$\frac{x(z)}{l_c} = \operatorname{arccosh}\left(\frac{2l_c}{z}\right) - \operatorname{arccosh}\left(\frac{2l_c}{h}\right) - \sqrt{4 - \frac{z^2}{l_c^2}} + \sqrt{4 - \frac{h^2}{l_c^2}} \quad (3)$$

where x denotes the distance to the vertical wall, z denotes the elevation of the profile above the level infinitely far from the wall, and $h \equiv z(x = 0)$ denotes the contact height. See refs 13 and 14 for an extended description.

Samples for this purpose were prepared by placing about 1 mL of the isolated bottom phases in disposable polystyrene cuvettes (1 × 1 cm^2) and carefully placing the same volume of isolated upper phases on top of them. The cuvettes were centrifuged for about 2 h at 200*g* to remove droplets that might have been formed as part of this procedure and afterward observed in a Nikon Eclipse LV100 Pol that had been rotated 90° to have a horizontal optical path. The profiles of the water−water interface were extracted using image recognition techniques and fitted to eq 3. An example is shown in Figure 1.

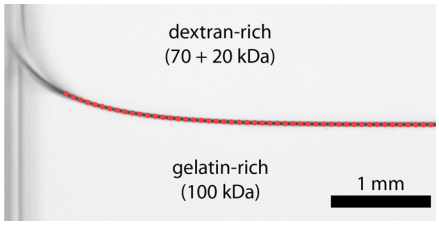

Figure 1. Example of a profile of a water−water interface near a vertical cuvette wall (located on the left). The system is composed for 5.00, 2.50, and 5.00% of 70 kDa dextran, 20 kDa dextran, and 100 kDa gelatin, respectively, and has a tie-line length of L = 15.39 ± 0.06% as measured from optical rotation. The red dotted curve indicates the fit to eq 3, resulting in l_c = 0.710 ± 0.016 mm. Together with $\Delta\rho$ = 2.668 g L^{-1}, the application of eq 2 results in γ = 13.2 ± 0.6 μN m^{-1}.

Finally, the density of each phase was measured on an Anton Paar DMA 5000 oscillating U-tube density meter (accurate to 10^{-6} g cm^{-3}), such that the density difference of order 10^{-3} g cm^{-3} between the phases could be determined and the value of the interfacial tension could be inferred from the capillary length via eq 2. For each sample, four micrographs were analyzed and the results averaged.

Self-Consistent Field Computations. In this section, a brief outline of the self-consistent field (SCF) computations will be given. We employ the numerical lattice approximation

DOI: 10.1021/acs.jpcb.7b09967
J. Phys. Chem. B 2018, 122, 3354−3362

by Scheutjens and Fleer (SF-SCF), which is a versatile tool for computing the thermodynamic properties of, e.g., polymer, surfactant, and polyelectrolyte solutions at solid−liquid or liquid−liquid interfaces. In essence, it is an extension of Flory−Huggins theory[7] to include gradients. For a detailed background on this approach, we refer to other publications.[28,34−36] We used SF-SCF theory as implemented by the SFBox software package.[36]

In SF-SCF, the system is represented by lattice sites and molecules are composed of one or more segments, with one segment exactly filling one lattice site. It is a mean-field approach in which each segment interacts with an average potential due to the other segments; the objective of SCF is to obtain concentration profiles that are self-consistent and to minimize the free energy for a given system. Various geometries are possible, such as planar, cylindrical, or spherical, with gradients in one, two, or three dimensions. In the present work, the focus is on a flat interface, so we consider a planar geometry with gradients in one direction (x-axis).

To model the experimental system, our SCF computations involve two polymers A and B dissolved in a theta solvent (S), i.e., the Flory−Huggins interaction parameter is $\chi_{AS} = \chi_{BS} = 0.5$. Polymer A consists of $M_A = 1000$ or 300 monomers (to model the large and small dextrans, respectively), polymer B consists always of $M_B = 1000$ monomers, and the solvent consists of a single monomer ($M_S = 1$). These polymers will be denoted A_{1000}, A_{300}, and B_{1000} for short. Monomers A and B are mutually slightly repulsive, $\chi_{AB} = 0.05$, leading to phase separation above the critical point located at volume fractions $\phi_A = \phi_B \simeq 0.022$ for the system $A_{1000} + B_{1000}$. For the systems $A_{1000} + B_{1000}$ and $A_{300} + B_{1000}$, the ratio in the global volume fractions ϕ_A:ϕ_B was 1:1, and for the system $A_{1000} + A_{300} + B_{1000}$, the ratio in the global volume fractions was 2:1:2, to mimic our experiments. To compare with experiments, it is customary to set the length of a lattice site (corresponding to a single segment) equal to b = 0.3 nm.[36] Computations for systems relatively far from the critical point were carried out with 500 lattice layers, whereas closer to the critical point 1500 lattice layers were used, with mirrors placed before the first and after the last lattice layer.

Relevant physical quantities can be extracted from the SCF computations. The tie-line length, for instance, is defined on the basis of the volume fraction profiles $\phi_i(x)$ as

$$L \equiv \{[\phi_A(-\infty) - \phi_A(+\infty)]^2 + [\phi_B(-\infty) - \phi_B(+\infty)]^2\}^{1/2} \quad (4)$$

where $\phi_i(\pm\infty)$ indicates the volume fraction of A or B monomers in the bulk. This means effectively that for polymer A, we take here the sum of both small and large polymers $[\phi_A(\pm\infty) = \phi_{A_{1000}}(\pm\infty) + \phi_{A_{300}}(\pm\infty)]$, if both are present, to match the experiments.

The volume fraction profiles also give insight into the interfacial excess of each component. This can be quantified by computing

$$\theta_i = \int_{-\infty}^{x_{Gibbs}} dx[\phi_i(x) - \phi_i(-\infty)] + \int_{x_{Gibbs}}^{+\infty} dx[\phi_i(x) - \phi_i(+\infty)] \quad (5)$$

where the distance x is normalized by the lattice size b. The interfacial excess can only be computed when the position x_{Gibbs} of the Gibbs dividing plane is fixed. Here we choose x_{Gibbs} such that the interfacial excess of polymer A is equal to that of polymer B, $\theta_A = \theta_B$ (in the situation that for polymer A both small and large polymer fractions are present, θ_A is defined as the sum $\theta_A = \theta_{A_{1000}} + \theta_{A_{300}}$). This definition has the advantage that the Gibbs plane coincides with the symmetry plane for a symmetrical system (e.g., $A_{1000} + B_{1000}$). From the interfacial excess θ_i, the polymer or solvent adsorption number density Γ_i can be calculated as

$$\Gamma_i = \frac{\theta_i}{M_i b^2} \quad (6)$$

where M_i is the degree of polymerization of component i. It should be noted that, regardless of the choice for the location of the Gibbs plane, the sum $\sum_i \theta_i$ for all components i including the solvent must equal zero, because $\sum_i \phi_i(x)$ must equal unity at every position x. One may wonder why we did not choose the location of the Gibbs dividing plane such that the excess of the *solvent* is zero. The reason is that, for a symmetric system ($A_{1000} + B_{1000}$), the concentration of solvent in both bulk phases is equal, while *at* the interface the concentration of solvent is higher than in bulk to reduce unfavorable interactions between A and B.[13,37,38] Therefore, for such a system, the excess of solvent will always be positive and, in fact, independent of the position of the Gibbs plane. Since our computations start from (and include) the symmetric case, we choose not to use the definition of zero interfacial excess of solvent.

It is important to realize that the amount of polymer adsorbed depends on the volume available to the polymer in the bulk phase due to the influence of the translational entropy of the polymers.[39] This effect depends on polymer bulk concentration and the polymer length (distribution) and therefore may be a factor in polydisperse systems. Experiments have shown that this effect is most important when the polymer solution is dilute.[39] In our experiments, the polymer concentration is close to the overlap concentration so that we expect this effect to be small. This is also true for the self-consistent field calculations carried out, and it was explicitly verified that the bulk volume (the number of lattice layers) was always chosen large enough so that all properties (adsorptions, density profiles) are independent of the number of lattice layers.

The interfacial tension γ is equal to the excess grand potential Ω^{ex} per unit area A, which is in turn derived from the excess Helmholtz free energy F^{ex} obtained from the SCF computations. It is given by[1,40]

$$\gamma = \frac{\Omega^{ex}}{A} = \frac{1}{A}\left(F^{ex} - \sum_i \mu_i N_i^{ex}\right) \quad (7)$$

where μ_i is the chemical potential and N_i^{ex} is the excess number of molecules of type i.

RESULTS AND DISCUSSION

In this section, results from our experiments and self-consistent field computations are described and discussed. First, phase diagrams and results for the interfacial tensions are presented. Subsequently, interfacial density profiles are shown and discussed in terms of the interfacial excess of the components. Finally, the relation between interfacial excess and interfacial tension is discussed in terms of the Gibbs adsorption equation.

DOI: 10.1021/acs.jpcb.7b09967
J. Phys. Chem. B 2018, 122, 3354−3362

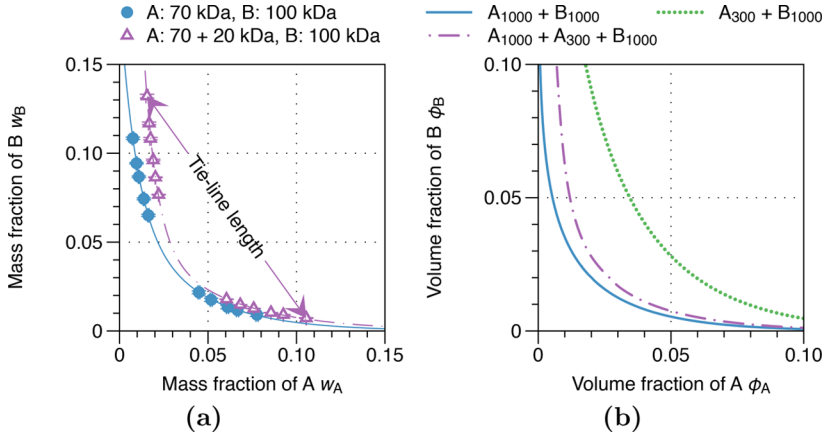

Figure 2. Effect on the phase diagram of adding a small polymer to a mixed solution of two larger polymers. (a) Phase diagrams from experiments on mixed aqueous solutions of dextran (labeled as polymer A) and gelatin (polymer B). The systems consist of dextran (70 kDa) with gelatin (100 kDa) in a 1:1 mass ratio and dextran (70 kDa) plus dextran (20 kDa) with gelatin (100 kDa) in a 2:1:2 mass ratio. The points indicate the measured coexisting phases, and the curves are to guide the eye. (b) Phase diagrams from self-consistent field computations for polymers A (degree of polymerization M_A = 1000 and/or 300) and B (M_B = 1000) in a theta solvent, with interaction parameter χ_{AB} = 0.05. The systems consist of two large polymers (A_{1000} + B_{1000}, 1:1 global volume fraction ratio), two large polymers plus small polymer (A_{1000} + A_{300} + B_{1000}, 2:1:2), and one small plus one large polymer (A_{300} + B_{1000}, 1:1, shown as a reference).

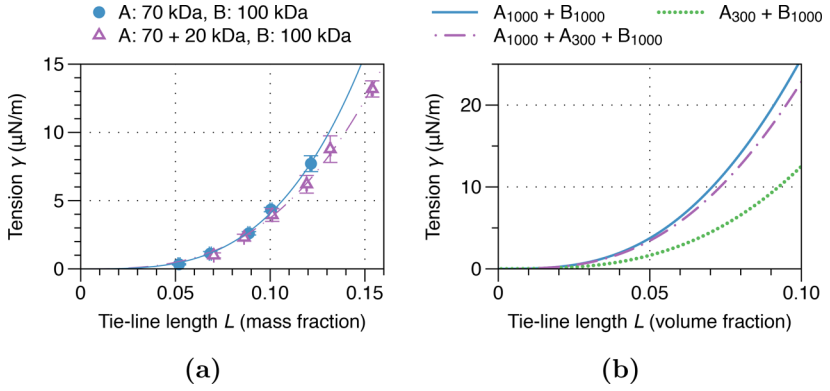

Figure 3. Effect of a small polymer on the interfacial tension of a mixed solution of two larger polymers from (a) experiments and (b) self-consistent field computations. The systems are the same as those in Figure 2.

Phase diagrams from experiments and SCF computations are shown in Figure 2 for a mixture of polymers A and B. In the experiments, the mass density of the pure polymers is about 1.5 g cm^{-3};[41] therefore, the range of the mass fraction axes in Figure 2a is directly comparable to the range of the volume fraction axes in Figure 2b. When additionally a smaller variant of polymer A is introduced to the system, the binodal is shifted away from the vertical axis in the phase diagram. This indicates that, although small polymer A does preferentially situate in the A-rich phase, significant amounts of small polymer A do remain in the B-rich phase. The agreement between experiment and SCF computations is near-quantitative. As evidenced from Figure 2b, we remain well below the concentrations where a system of only small polymer A and (large) polymer B would phase separate, as the compatibility generally increases with decreasing polymer molar mass.[7]

In Figure 3, corresponding interfacial tensions are shown as a function of the tie-line length L (defined graphically in Figure 2a). There is a modest difference in the absolute magnitudes of the tension between experiment and theory, but the trends are almost quantitatively the same: a systematic decrease of about 10% of the tension occurs upon addition of a small polymer for systems of equal tie-line length. For the SCF computations, the tension of the system composed of only small polymer A and large polymer B is also shown as a reference, and the interfacial tension is about 40−50% lower in that scenario. This is consistent with the observation that the interfacial tension decreases with decreasing degree of polymerization at fixed tie-line length.[42,43]

The interfacial tension is further investigated in Figure 4, where the ratio of the tension γ with respect to the tension γ_0 of the system containing only two large polymers is plotted for the SCF computations. Interestingly, while for the system A_{300} + B_{1000} the relative tension *increases* with increasing tie-line length, for the system A_{1000} + A_{300} + B_{1000} the relative tension *decreases*. In other words, it appears that the effect of polydispersity on the interfacial tension as modeled by the addition of the smaller polymer component is stronger at larger tie-line lengths and that, in this sense, the effect is quantitatively different from just a decrease in the average degree of polymerization. This point is addressed in more detail in a later part of this section. It is not possible to create a plot such as in Figure 4 with the same accuracy for the experiment results, but we estimate that on average $\gamma/\gamma_0 \approx 0.89$, very similar to the SCF computations.

DOI: 10.1021/acs.jpcb.7b09967
J. Phys. Chem. B 2018, 122, 3354−3362

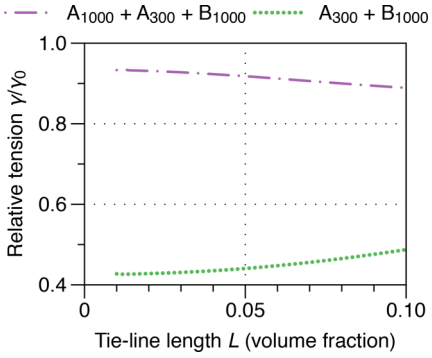

Figure 4. Interfacial tensions γ from Figure 3b of systems $A_{1000} + A_{300} + B_{1000}$ and $A_{300} + B_{1000}$ relative to the tension γ_0 of the system of two large polymers $A_{1000} + B_{1000}$.

In order to investigate whether the addition of small polymers to a high molar mass system leads to a higher or lower interfacial tension, one should in some way take the fact into account that the phase diagram itself depends on the polymer chain length. Therefore, to account for the shift in the location of the critical point, we elected to compare results at equal tie-line length. We found that the small polymers adsorb at the interface, leading to a small but significant lowering of the interfacial tension consistent with our self-consistent field calculations. Still, it could be questioned whether the tie-line length is the most appropriate way of comparing different systems. Another method would be to scale the polymer concentrations with their critical concentrations, for instance, but this requires a very precise determination of the polymer concentrations at the critical point to avoid systematic errors. This is, however, experimentally especially difficult. The tie-line length has the advantage that it does not require normalization and is easily accessible experimentally for our system. Additionally, comparing systems at equal tie-line length ensures that on average the concentration differences across the interface are the same, ensuring that the density profiles (and interfacial widths) are similar.

We now turn our attention to the interfacial density profiles and the corresponding interfacial excesses of the various components. Density profiles from SCF computations are shown in Figure 5a for a tie-line length of $L = 0.070$. It is clear, especially in the top and bottom panels, that the polymers are *depleted* from the interface and that there is a local excess of *solvent*. The reason for this phenomenon lies in the fact that unfavorable contacts between polymers A and B at the interface are reduced in this way. The result is also that the interfacial tension is significantly reduced compared to the hypothetical scenario in which the density of solvent across the interface would be constant.[13,37,38] It is also clear that small polymer A, when in both the absence and presence of large polymer A, shows much weaker partitioning over the two phases. Additionally, the phase that is enriched in small polymer A contains more solvent due to the higher osmotic pressure of the smaller polymer.

By normalizing all volume fractions such that they are zero in one bulk phase and unity in the other bulk phase ($\bar{\phi}_i(x) = [\phi_i(x) - \phi_i(\mp\infty)]/[\phi_i(\pm\infty) - \phi_i(\mp\infty)]$), it becomes apparent that, for the system $A_{1000} + A_{300} + B_{1000}$, the small polymer A extends significantly into the B-rich phase. For

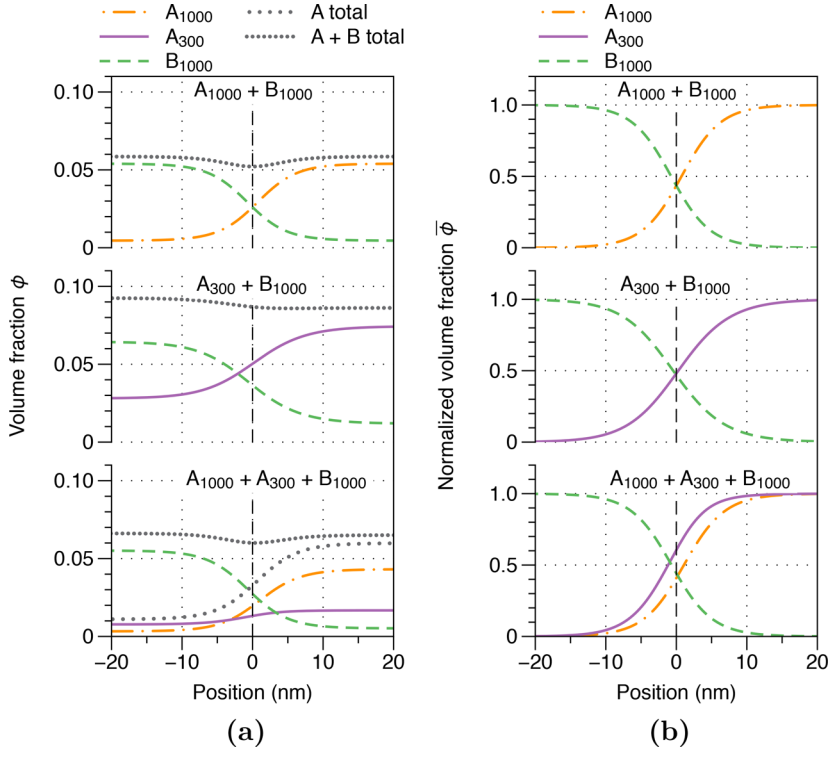

Figure 5. Density profiles from self-consistent field computations for a mixed solution of two large polymers ($A_{1000} + B_{1000}$), a small and a large polymer ($A_{300} + B_{1000}$), and two large polymers mixed with one small polymer ($A_{1000} + A_{300} + B_{1000}$, 2:1:2 volume ratio). The profiles are centered around the Gibbs dividing plane (dashed vertical lines) located such that the interfacial excesses of polymers A and B are equal. The tie-line length is $L = 0.070$ in all cases. The interfacial tension is $\gamma = 9.74$, 4.47, and 8.82 μN m^{-1} (top to bottom). The density profiles are expressed as (a) volume fractions and (b) normalized volume fractions ($\bar{\phi}_i(x) = [\phi_i(x) - \phi_i(\mp\infty)]/[\phi_i(\pm\infty) - \phi_i(\mp\infty)]$).

DOI: 10.1021/acs.jpcb.7b09967
J. Phys. Chem. B 2018, 122, 3354−3362

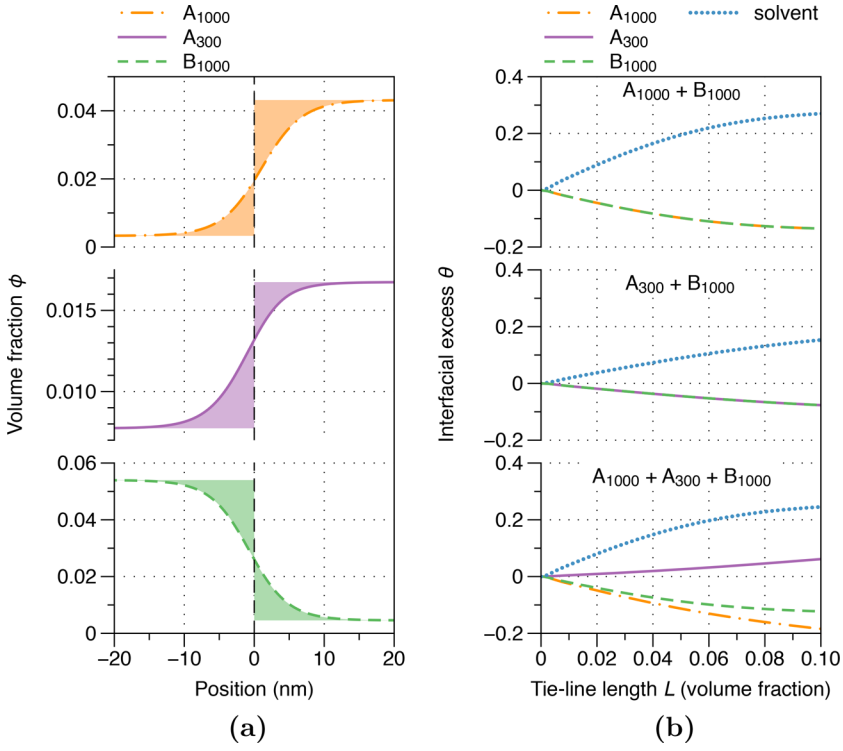

Figure 6. Interfacial excesses from self-consistent field computations for a mixed solution of two large polymers (A_{1000} + B_{1000}), a small and a large polymer (A_{300} + B_{1000}), and two large polymers mixed with one small polymer (A_{1000} + A_{300} + B_{1000}, 2:1:2 volume ratio). (a) Definition of the Gibbs dividing plane (dashed vertical lines), using the profiles for the system A_{1000} + A_{300} + B_{1000} from Figure 5a as an example. The Gibbs plane is located such that the excess (filled regions) of polymers A_{1000} and A_{300} in total is equal to that of polymer B_{1000}. (b) The interfacial excess θ_i as defined in eq 5 for each component, computed from density profiles such as those in part a with the Gibbs dividing plane as indicated.

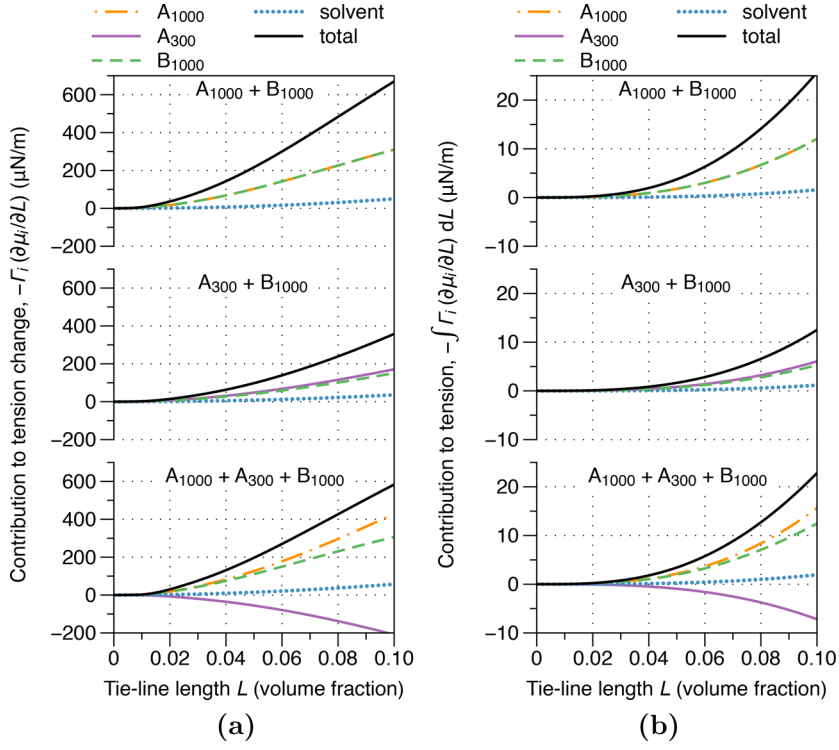

Figure 7. Contributions to the interfacial tension according to the Gibbs adsorption equation, from self-consistent field computations for a mixed solution of two large polymers (A_{1000} + B_{1000}), a small and a large polymer (A_{300} + B_{1000}), and two large polymers mixed with one small polymer (A_{1000} + A_{300} + B_{1000}, 2:1:2 volume ratio). (a) Contribution to the change $\partial\gamma/\partial L$ of the interfacial tension with tie-line length, according to $-\Gamma_i(\partial\mu_i/\partial L)$. (b) Integrated contributions to the interfacial tension, $-\int\Gamma_i(\partial\mu_i/\partial L)\,dL$.

DOI: 10.1021/acs.jpcb.7b09967
J. Phys. Chem. B 2018, 122, 3354−3362

Figure 5a, the result of this procedure is shown in Figure 5b. It turns out that the profile of A_{300} is shifted about 2.4 nm (or eight lattice layers) toward the B-rich phase with respect to A_{1000}; this shift is only weakly dependent on the tie-line length. (A quantitative way to arrive at this number is by computing the first moment of the derivative of $\phi_i(x)$ with respect to position, $x_{1,i} = [\int_{-\infty}^{+\infty} x\phi_i'(x)\,dx]/[\int_{-\infty}^{+\infty} \phi_i'(x)\,dx]$.)

It is interesting to investigate this in more detail by determining the interfacial excess θ_i of all components as defined in eq 5 and sketched in Figure 6a. The result is shown in Figure 6b as a function of the tie-line length. The interfacial excess of solvent is always positive; therefore, the excess of the polymers is, in total, always negative. Compared to the system A_{1000} + B_{1000}, the magnitudes of the excesses are somewhat smaller for A_{300} + B_{1000}. When both A_{1000} and A_{300} are present, the small component shows positive adsorption, in line with the reasoning in the previous paragraph, at the expense of a slightly reduced adsorption of solvent. Naturally, the exact magnitude of the interfacial excess depends on the precise definition of the Gibbs plane; however, the (relative) trends remain similar, as the sum of the excesses θ_i must remain zero.

At first glance, it may seem surprising that the system partially exchanges a positive excess of solvent for a positive excess of small polymer to decrease the interfacial tension. After all, according to the Gibbs adsorption equation

$$d\gamma = -\sum_i \Gamma_i\, d\mu_i \tag{8}$$

the change of the interfacial tension is proportional to the adsorption *density* Γ_i, in units of number of molecules per unit area. If the decrease in θ_i for the solvent is similar to the increase for the small polymer, then the decrease in Γ_i for the solvent is orders of magnitude larger than the increase for the small polymer (see eq 6, where $M_S = 1$ and $M_{A_{300}} = 300$). It may therefore appear that this exchange should only *increase* the interfacial tension, but obviously, from Figure 3, we know that the tension must decrease. To resolve this apparent contradiction, we consider the implications of the Gibbs adsorption equation in more detail.

Let us consider the dependence of the interfacial tension as a function of the position in the phase diagram, i.e., as a function of the tie-line length L. According to eq 8, this leads to

$$\frac{\partial\gamma}{\partial L} = -\sum_i \Gamma_i \frac{\partial\mu_i}{\partial L} \tag{9}$$

By taking the (numerical) derivative of the chemical potential μ_i, known from the SCF computations, with respect to the tie-line length L, we can assess the relative importance of the excess of each component. After multiplication with $-\Gamma_i$, we find the relative contribution of each component to $\partial\gamma/\partial L$. The result of this procedure is shown in Figure 7a.

For the polymers, $\partial\mu_i/\partial L > 0$, because μ_i increases with ϕ_i as the systems are in thermodynamic equilibrium and ϕ_i in turn increases with L. Combined with a negative excess, this results in a positive contribution to the change $\partial\gamma/\partial L$ of tension with tie-line length. There is one important exception, however: the small polymer in the system A_{1000} + A_{300} + B_{1000} shows positive adsorption and therefore contributes *negatively* to the increase of the tension with the tie-line length (Figure 7a, bottom panel).

In contrast, as the concentration of *solvent* decreases with increasing L, we have that $\partial\mu_S/\partial L < 0$. This means that, even though the solvent shows a positive interfacial excess, it still has a *positive* contribution to the increase of γ with tie-line length, just as for the polymers. Additionally, because the solvent has a very large volume fraction by comparison, the *relative* change of ϕ_S with L is small, and by extension, $\partial\mu_S/\partial L$ is so small that the solvent hardly contributes to $\partial\gamma/\partial L$, see Figure 7a, even though $|\Gamma_i|$ is orders of magnitude larger for the solvent than for the other components. This negligible change in the chemical potential of the solvent is the reason why the positive excess of A_{300} decreases the interfacial tension and that, in fact, this positive excess exists in the first place.

One may verify that the interfacial tension in Figure 3b is reproduced when eq 9 is integrated numerically from the critical point, where $\gamma = 0$ and $L = 0$,

$$\gamma(L) = \int_0^L \frac{\partial\gamma}{\partial L'}\,dL' = -\sum_i \int_0^L \Gamma_i \left(\frac{\partial\mu_i}{\partial L'}\right) dL' \tag{10}$$

One of the advantages of calculating γ using eq 10 is that it provides a means to analyze the contribution of each component to the tension separately (see Figure 7b). First, it is noted that all contributions to γ scale in the same way near the critical point, i.e., $\gamma \propto L^{\mu/\beta} \propto L^3$, where the exponents μ and β are equal to their mean-field values $\mu = 3/2$ and $\beta = 1/2$, as expected.[1] Second, it is apparent that the contributions of the two large polymers and solvent are very similar for the systems in the top and bottom panels of Figure 7b, and therefore not strongly affected by the presence of the small polymer.

It is also visible that the negative contribution of A_{300} to the interfacial tension increases relatively with tie-line length. This is likely driven by a continued increase in the interfacial excess θ_i of the small polymer in Figure 6b (bottom panel) at larger tie-line lengths, while the excess of the other components gradually levels off. We believe that this elucidates the mechanism for the phenomenon observed in Figure 4, where the relative tension γ/γ_0 decreased with the tie-line length for the system of two large polymers with one small polymer: the adsorption of the small polymer is most pronounced at larger tie-line lengths.

The self-consistent field calculations have shown that the decrease in interfacial tension is related to a weak but positive adsorption of the smaller polymer, which leads us to believe that this effect is behind the same decrease observed in experiments. Therefore, it would be interesting to understand this enhanced adsorption also on a molecular level. In that case, one should consider many molecular factors such as the adsorption enthalpy, the loss of translational entropy, the entropy associated with the dangling chain ends, etc. Since these effects all depend on polymer chain length, concentration, and composition, such a molecular description is rather complicated for the system at hand, and we leave it for future work.

CONCLUSIONS

We have investigated solutions of two incompatible polymers A and B containing a fraction with significantly lower degree of polymerization using experiments and self-consistent field computations. Phase diagrams from both experiments and theory show that the fraction of smaller polymer participates weakly in the phase separation. Comparing systems at equal tie-line length, a decrease in the interfacial tension is observed. An analysis based on the Gibbs adsorption equation of our self-consistent field computations shows that this decrease is driven

DOI: 10.1021/acs.jpcb.7b09967
J. Phys. Chem. B 2018, 122, 3354−3362

by positive adsorption of the small polymer and that the effect is most prominent at larger tie-line lengths. We believe that our approach may serve as a model to comprehend better the effect of polydispersity, a ubiquitous phenomenon in practical systems, on the interfacial structure and interfacial tension of incompatible polymer solutions.

AUTHOR INFORMATION

Corresponding Author

*E-mail: M.Vis@tue.nl.

ORCID

Mark Vis: 0000-0002-2992-1175

Notes

The authors declare no competing financial interest.

ACKNOWLEDGMENTS

M.V. would like to thank Prof. R. Tuinier for fruitful discussions. There are no funding agencies to disclose for this work.

REFERENCES

(1) Widom, B.; Rowlinson, J. S. *Molecular Theory of Capillarity*; Oxford University Press: Oxford, 1984.

(2) van der Waals, J. D. Over de continuiteit van den gas- en vloeistoftoestand. Ph.D. Thesis, Leiden University, 1873.

(3) van der Waals, J. D. Thermodynamische theorie der capillariteit in de onderstelling van continue dichtheidsverandering. *Verhandel. Konink. Akad. Weten., Amsterdam (Sect. 1)* **1893**, *1*, 1−56.

(4) Cahn, J. W.; Hilliard, J. E. Free energy of a nonuniform system. I. Interfacial free energy. *J. Chem. Phys.* **1958**, *28*, 258−267.

(5) Evans, R. Nature of the liquid-vapor interface and other topics in Statistical Mechanics of non-uniform, classical fluids. *Adv. Phys.* **1979**, *28*, 143−200.

(6) Widom, B. What do we know that van der Waals did not know? *Phys. A* **1999**, *263*, 500−515.

(7) Flory, P. J. *Principles of Polymer Chemistry*; Cornell University Press: Ithaca, NY, 1953.

(8) Dee, G. T.; Sauer, B. B. The surface tension of polymer liquids. *Adv. Phys.* **1998**, *47*, 161−205.

(9) Capron, I.; Costeux, S.; Djabourov, M. Water in water emulsions: phase separation and rheology of biopolymer solutions. *Rheol. Acta* **2001**, *40*, 441−456.

(10) Edelman, M. W.; van der Linden, E.; de Hoog, E. H. A.; Tromp, R. H. Compatibility of gelatin and dextran in aqueous solution. *Biomacromolecules* **2001**, *2*, 1148−1154.

(11) Guido, S.; Simeone, M.; Alfani, A. Interfacial tension of aqueous mixtures of Na-caseinate and Na-alginate by drop deformation in shear flow. *Carbohydr. Polym.* **2002**, *48*, 143−152.

(12) Scholten, E.; Tuinier, R.; Tromp, R. H.; Lekkerkerker, H. N. W. Interfacial tension of a decomposed biopolymer Mixture. *Langmuir* **2002**, *18*, 2234−2238.

(13) Vis, M.; Peters, V. F. D.; Blokhuis, E. M.; Lekkerkerker, H. N. W.; Erné, B. H.; Tromp, R. H. Effects of electric charge on the interfacial tension between coexisting aqueous mixtures of polyelectrolyte and neutral polymer. *Macromolecules* **2015**, *48*, 7335−7345.

(14) Vis, M.; Peters, V. F. D.; Blokhuis, E. M.; Lekkerkerker, H. N. W.; Erné, B. H.; Tromp, R. H. Decreased interfacial tension of demixed aqueous polymer solutions due to charge. *Phys. Rev. Lett.* **2015**, *115*, 078303.

(15) Nguyen, B. T.; Nicolai, T.; Benyahia, L. Stabilization of water-in-water emulsions by addition of protein particles. *Langmuir* **2013**, *29*, 10658−10664.

(16) Vis, M.; Opdam, J.; van't Oor, I. S. J.; Soligno, G.; van Roij, R.; Tromp, R. H.; Erné, B. H. Water-in-water emulsions stabilized by nanoplates. *ACS Macro Lett.* **2015**, *4*, 965−968.

(17) Helfand, E.; Bhattacharjee, S. M.; Fredrickson, G. H. Molecular weight dependence of polymer interfacial tension and concentration profile. *J. Chem. Phys.* **1989**, *91*, 7200−7208.

(18) Ermoshkin, A.; Semenov, A. Interfacial tension in binary polymer mixtures. *Macromolecules* **1996**, *29*, 6294−6300.

(19) Szleifer, I.; Widom, B. Structure and tension of the interface between dilute polymer solutions. *J. Chem. Phys.* **1989**, *90*, 7524−7534.

(20) Xia, K.-Q.; Franck, C.; Widom, B. Interfacial tensions of phase-separated polymer solutions. *J. Chem. Phys.* **1992**, *97*, 1446−1454.

(21) Widom, B. Phase separation in polymer solutions. *Phys. A* **1993**, *194*, 532−541.

(22) Koningsveld, R.; Kleintjens, L. A.; Schoffeleers, H. M. Thermodynamic aspects of polymer compatibility. *Pure Appl. Chem.* **1974**, *39*, 1−32.

(23) Edelman, M. W.; Tromp, R. H.; van der Linden, E. Phase-separation-induced fractionation in molar mass in aqueous mixtures of gelatin and dextran. *Phys. Rev. E: Stat. Phys., Plasmas, Fluids, Relat. Interdiscip. Top.* **2003**, *67*, 021404.

(24) Shresth, R. S.; McDonald, R. C.; Greer, S. C. Molecular weight distributions of polydisperse polymers in coexisting liquid phases. *J. Chem. Phys.* **2002**, *117*, 9037−9049.

(25) Fairhurst, D. J.; Evans, R. M. L. De-mixing of polydisperse fluids: experimental test of a universal relation. *Colloid Polym. Sci.* **2004**, *282*, 766−769.

(26) Forciniti, D.; Hall, C. K.; Kula, M. R. Influence of polymer molecular-weight and temperature on phase-composition in aqueous 2-phase systems. *Fluid Phase Equilib.* **1991**, *61*, 243−262.

(27) Broseta, D.; Leibler, L.; Joanny, J. F. Critical properties of incompatible polymer blends dissolved in a good solvent. *Macromolecules* **1987**, *20*, 1935−1943.

(28) Scheutjens, J. M. H. M.; Fleer, G. J. Statistical theory of the adsorption of interacting chain molecules. 1. Partition function, segment density distribution, and adsorption isotherms. *J. Phys. Chem.* **1979**, *83*, 1619−1635.

(29) Tromp, R. H.; ten Grotenhuis, E.; Olieman, C. Self-aggregation of gelatine above the gelling temperature analysed by SEC-MALLS. *Food Hydrocolloids* **2002**, *16*, 235−239.

(30) Kasapis, S.; Morris, E. R.; Norton, I. T.; Gidley, M. J. Phase equilibria and gelation in gelatin/maltodextrin systems—Part II: Polymer incompatibility in solution. *Carbohydr. Polym.* **1993**, *21*, 249−259.

(31) Vis, M.; Peters, V. F. D.; Tromp, R. H.; Erné, B. H. Donnan potentials in aqueous phase-separated polymer mixtures. *Langmuir* **2014**, *30*, 5755−5762.

(32) Aarts, D. G. A. L.; van der Wiel, J. H.; Lekkerkerker, H. N. W. Interfacial dynamics and the static profile near a single wall in a model colloid-polymer mixture. *J. Phys.: Condens. Matter* **2003**, *15*, S245−S250.

(33) Batchelor, G. K. *An introduction to fluid dynamics*; Cambridge University Press: Cambridge, U.K., 2002.

(34) Fleer, G. J.; Cohen Stuart, M. A.; Scheutjens, J. M. H. M.; Cosgrove, T.; Vincent, B. *Polymers at interfaces*; Chapman and Hall: London, 1993.

(35) Leermakers, F. A. M.; Eriksson, J. C.; Lyklema, J. In *Fundamentals of interface and colloid science*; Lyklema, J., Ed.; Elsevier: Amsterdam, The Netherlands, 2005; Vol. 5, Chapter 4.

(36) van Male, J. Self-consistent-field theory for chain molecules: extensions, computational aspects, and applications. Ph.D. Thesis, Wageningen University, 2003.

(37) Tromp, R. H.; Blokhuis, E. M. Tension, rigidity, and preferential curvature of interfaces between coexisting polymer solutions. *Macromolecules* **2013**, *46*, 3639−3647.

(38) Broseta, D.; Leibler, L.; Kaddour, L. O.; Strazielle, C. A theoretical and experimental study of interfacial tension of immiscible polymer blends in solution. *J. Chem. Phys.* **1987**, *87*, 7248.

(39) Koopal, L. The effect of polymer polydispersity on the adsorption isotherm. *J. Colloid Interface Sci.* **1981**, *83*, 116−129.

DOI: 10.1021/acs.jpcb.7b09967
J. Phys. Chem. B 2018, 122, 3354−3362

(40) Leermakers, F. A. M.; Eriksson, J. C.; Lyklema, J. In *Fundamentals of interface and colloid science: soft colloids*; Lyklema, J., Ed.; Academic Press: Amsterdam, 2005; Vol. 5.
(41) Vis, M. Interfacial thermodynamics of coexisting aqueous polymer solutions. Ph.D. Thesis, Utrecht University, 2015.
(42) Forciniti, D.; Hall, C. K.; Kula, M. R. Interfacial tension of polyethyleneglycol-dextran-water systems: influence of temperature and polymer molecular weight. *J. Biotechnol.* **1990**, *16*, 279−296.
(43) Ding, P.; Wolf, B.; Frith, W. J.; Clark, A. H.; Norton, I. T.; Pacek, A. W. Interfacial tension in phase-separated gelatin/dextran aqueous mixtures. *J. Colloid Interface Sci.* **2002**, *253*, 367−376.

DOI: 10.1021/acs.jpcb.7b09967
J. Phys. Chem. B 2018, 122, 3354−3362